NATIONAL UNIVERSITY OF SCIENCE AND TECHNOLOGY **POLITEHNICA** OF BUCHAREST

Doctoral School of Electrical Engineering

Doctoral Thesis

Electromagnetic Methods in Biomedical Processes Study

- Summary -

Author: *MSc. Eng.* ***Sorina GOGONEAȚĂ***

Scientific coordinator: *Prof. PhD. Eng.* ***Alexandru Mihail MOREGA***

Bucharest

2023

Content

Keywords: *electromagnetic field, biosensor, 3D printed electrodes, Electrochemical Impedance Spectroscopy (EIS), microfluidic structures, Lab-on-chip, finite elements, multiphysics models*

CHAPTER 1 - INTRODUCTION

1.1. PROBLEM FORMULATION

Understanding electromagnetic fields in the biomedical environment is essential in various situations, including their interaction with biological systems and electromagnetic interference with medical devices.

The aim of the research in this thesis is to investigate the interaction of electromagnetic fields with the biological environment within biosensors, taking into consideration electrochemical detection, electrochemical behavior modeling, and sensor integration into microfluidic platforms.

To achieve the stated objective, the research focuses on two main directions, which are essential for the development of the doctoral thesis. These directions are:

- *The electrochemical detection problem* is based on changes in the electric field or electrical properties of the working medium depending on the analyte concentration in biological samples. In Chapters 3 and 5, the use of impedance spectroscopy for detecting organic compounds in biological samples and modeling the electrochemical behavior of biological material and the metallic substrate of electrodes using equivalent electrical circuits is analyzed.
- *The integration of biosensors into microfluidic platforms*, which enable the manipulation of fluids on a small scale using electric fields, is addressed in Chapter 4. Complex microfluidic devices, such as Lab-on-a-Chip (LoC) systems, comprise multiple microchannels for controlled fluid dosing using microvalves and micropumps, as well as flow sensors and biofilters for flow control. The use of such devices allows the detection of biological reactions at the analyte interface with the microsensor surface, thereby eliminating the need for signal amplification in label-free biodetection.

1.2. RESEARCH OBJECTIVES

The overall objective of the thesis is to research and develop advanced methods and devices in the field of biosensors, with a focus on the interaction of electromagnetic fields with the biological environment. The aim is to gain detailed knowledge and understanding of field-substance interactions in these domains and to contribute to the advancement of research in this direction.

Within this thesis, significant *contributions have been made to the field of theoretical research* by elaborating and developing complex numerical models. These models were proposed with the purpose of investigating the effects of applying an electric field on fluid flow phenomena in microchannels and on mass transport processes in microfluidic systems.

This work also provides *practical contributions* through the development of an innovative electrode fabrication method using 3D printing, thus obtaining electrodes with precise shapes and dimensions tailored to the experimental requirements and needs in the field of biosensors. These electrodes are used for the detection and quantification of various biomolecules in the analyzed samples.

1.3. THESIS STRUCTURE AND CONTENT

Chapter 1 - Introduction: This chapter provides the context and significance of the research.

Chapter 2 - Current State of Impedimetric Biosensors: This chapter conducts a detailed analysis of the current state of research in the field of impedimetric biosensors and describes the main advances in this field.

Chapter 3 - Electrical Interactions and Processes in Biosensing Systems: This chapter explores biosensors, devices for analyzing biological material, with a focus on their operating principles and components.

Chapter 4 - Influence of Electric Fields on Fluid Flow in Microchannels, Applications of Electrochemical Biosensors: This chapter explores the applications of electrochemical biosensors in the detection and identification of DNA hybridization, with particular attention to the design of DNA biosensors integrated into a microfluidic device.

Chapter 5 - Characterization of Electrical Properties of 3D-Printed Electrodes: This chapter presents and analyzes the results related to the characterization of electrical properties of 3D-printed electrodes, with a focus on the development of electrochemical biosensors.

Chapter 6 - Conclusions: This chapter synthesizes and analyzes the research conducted, presenting relevant conclusions and perspectives obtained from the study.

CHAPTER 2 – CURRENT STATE OF IMPEDIMETRIC BIOSENSORS

2.1. ELECTROMAGNETIC METHODS IN THE STUDY OF BIOMEDICAL PROCESSES

The interaction between biological systems and electromagnetic fields has been addressed in numerous scientific papers and continues to be a subject of great interest for many researchers. These studies encompass the investigation of the electromagnetic field's interaction with biological tissues and living systems, as well as the development of diagnostic and treatment applications.

The study of biosensors involves characterizing the electrical properties of electrochemical biosensors manufactured through 3D printing technology. The aim is to understand the electrical response of these biosensors and evaluate their performance based on relevant electrical parameters, such as conductivity or electrical impedance.

Research on biosensors extends into the direction of integrating them into microfluidic platforms, representing an unconventional approach in simulating the environment in which biochemical processes occur, compared to traditional established methods.

The use of numerical modeling to simulate the electromagnetic properties of biological media contributes significantly to understanding and analyzing these complex environments. This approach allows researchers to explore the interaction between electromagnetic fields and biological media, providing a better understanding of the phenomena and processes involved in the study [1] .

2.2. BIOSENSORS

Biosensors are a category of devices that integrate advanced technologies from the fields of engineering and biotechnology. These devices can be used to monitor living systems and may incorporate biological elements [3] .

Biosensors allow the detection and measurement of the presence of specific molecules in an analyte. Within the biosensor, components or chemical species in the environment interact, and the biosensor detects these interactions, allowing for the identification and measurement of the concentration of the substance of interest.

Active electrical biosensors generate an electrical signal, such as voltage or current, in response to chemical reactions, such as the binding of two molecules, for example. These reactions or interference with electrical fields can cause changes in the electrical parameters of the biosensor [9] .

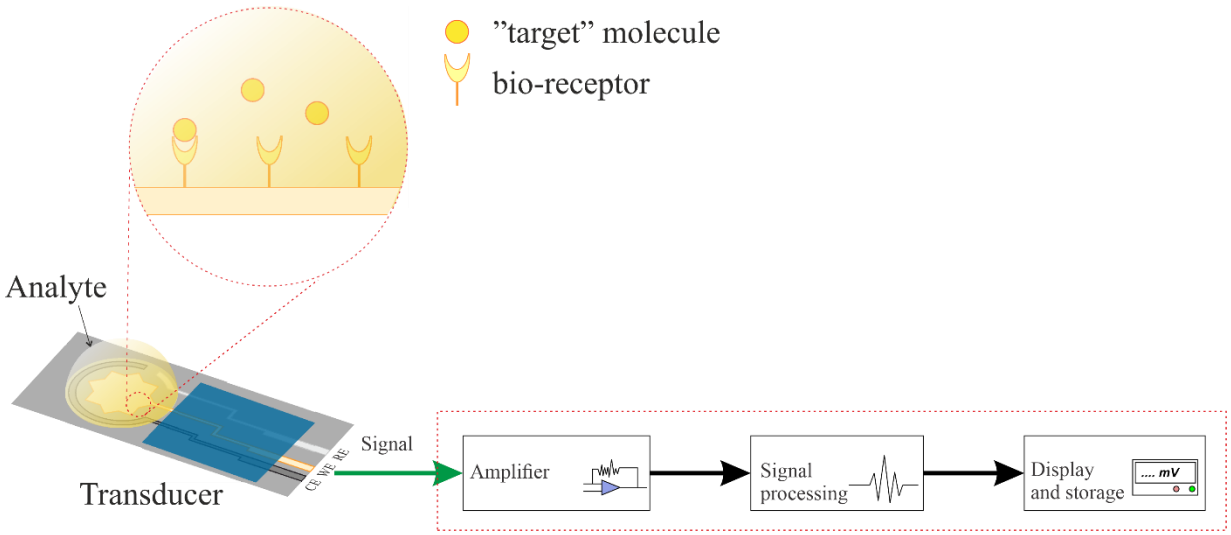

Fig. 2.1. The operating principle of a biosensor

According to the representation in Fig. 2.1, a biosensor consists of a biological receptor such as an enzyme, antibody, nucleic acid or cell, which binds to a specific component. The bio-receptor is associated with a transducer that converts the receptor-analyte interaction into a

measurable signal, using electrodes and electrical, thermal or optical systems, depending on the variations in the physical quantities being measured [3] .

In biosensor research, an essential element is the working electrode. The working electrode serves as the interface through which an electric field can be applied to the sample under study, allowing interaction with biological components, and it is also used for measuring and transmitting the detected electrical signals.

The characteristics of the obtained electrical signals are influenced by the type of biosensor and application: medical diagnostics, environmental monitoring, food safety or personal health monitoring. Measurements of resistance or capacitance can be performed, as well as electrical impedance spectroscopy within a certain range of frequencies [10] . In measuring the variation of electrical impedance to determine the concentration of certain biomolecules in an analyte, a proportional relationship can be established between the measured electrical impedance and the concentration of biomolecules in the analyte. This proportional relationship is represented through a standard curve [8] , which is a mathematical representation of the correlation between the measured electrical impedance and the known concentration of biomolecules in the analyte.

The electromagnetic field experiences significant changes within tissues compared to the external environment. The depth of penetration of the electromagnetic field into tissues is influenced by frequency and the characteristics of these tissues. The depth of penetration can vary considerably, ranging from a few millimeters to centimeters or even more, depending on the frequency of the electromagnetic field and the specific type of tissue [12] .

2.3. BIOSENSOR INTEGRATED INTO A MICROFLUIDIC PLATFORM

The study of the interaction between electromagnetic fields and biochemical processes under similar conditions to those in natural environment where these processes occur, provides relevant information for understanding the mechanisms through which electromagnetic fields influence these processes at the molecular and cellular levels. The integration of multiple laboratory analyses into a "lab-on-a-chip" (LOC) is a significant advancement in the field of biosensors. This concept allows for various tests and experiments to be conducted with small quantities of biological samples and reagents, with applications in personalized medicine, rapid diagnostics, and health monitoring.

In the investigation process, unknown species are guided close to the microchannel wall using various methods such as diffusion or electroosmotic flow. This allows their interaction with the detection surface represented in Fig. 2.2, facilitating their detection and characterization [14] .

Mass transfer through diffusion and osmosis is based on the diffusion equations and describes the movement of substances in relation to the concentration or pressure gradient.

For heat transfer, the law of conservation of energy is used. In the case of an LOC device, this means that the transfer of energy between the fluid and the electric field can affect the overall behavior of the system, but the total energy of the system is conserved.

Electromagnetic energy transfer is closely related to Maxwell's equations, as these equations describe the behavior of electromagnetic fields and the propagation of electromagnetic waves, and electromagnetic energy transfer occurs through these fields and waves.

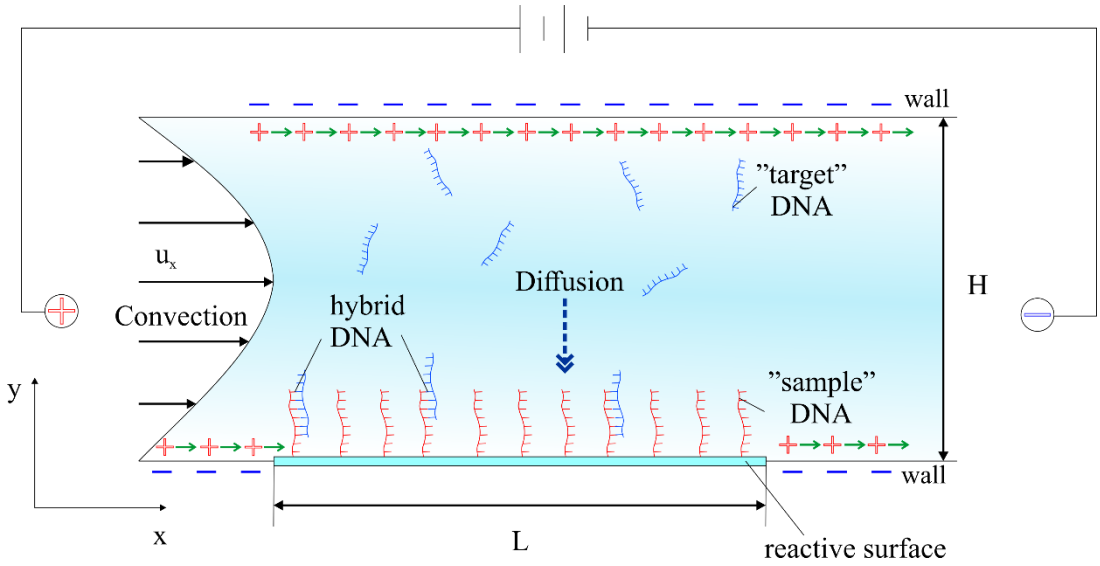

Fig. 2.2. The movement of DNA species near the microchannel wall

2.4. 3D-PRINTED IMPEDIMETRIC BIOSENSORS

Biosensors detect biological substances by generating detectable signals, and electrochemical impedance spectroscopy is a common method for analyzing these biodetection systems. Changes in the active area lead to variations in the measured impedance, reflecting changes in electrochemical processes and interactions at the electrode-electrolyte interface [16] .

To simplify the complex electrical phenomena in biosensors and enable an understanding of their operation, equivalent circuit models are used. The Randles-Sevcik circuit model represents the biosensor electrodes and their electrochemical behavior during the electron transfer reaction, as shown in Fig. 2.3.

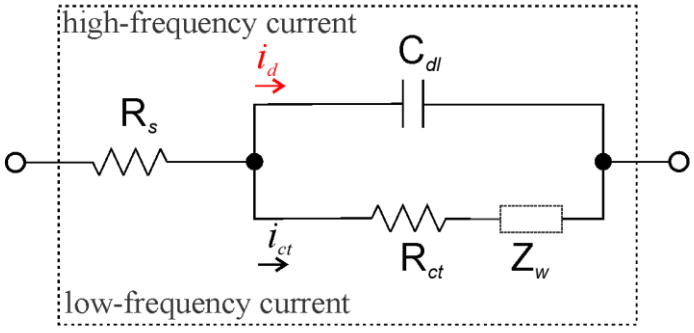

Fig. 2.3. The Randles-Sevcik equivalent circuit model [17]

In recent years, 3D printing technologies have gained significant importance in the development and manufacturing of biosensors. Specifically, these technologies have been widely used to create electrodes with complex shapes and geometries, which are essential for various

biodetection applications and in microfluidic systems. Complex-shaped electrodes can be optimized to enhance the sensitivity and selectivity of specific biomolecule detection.

CHAPTER 3 – INTERACTIONS AND ELECTRICAL PROCESSES IN BIOSENSOR-BASED BIODETECTION SYSTEMS

3.1. ELECTROMAGNETIC FILED EFFECTS BIOSENSORS – DEVICES FOR BIOLOGICAL MATERIAL ANALYSIS

Biosensors are capable of accurately detecting and measuring very small quantities of specific substances, which gives them high sensitivity for the analysis of biomolecules and various medical applications.

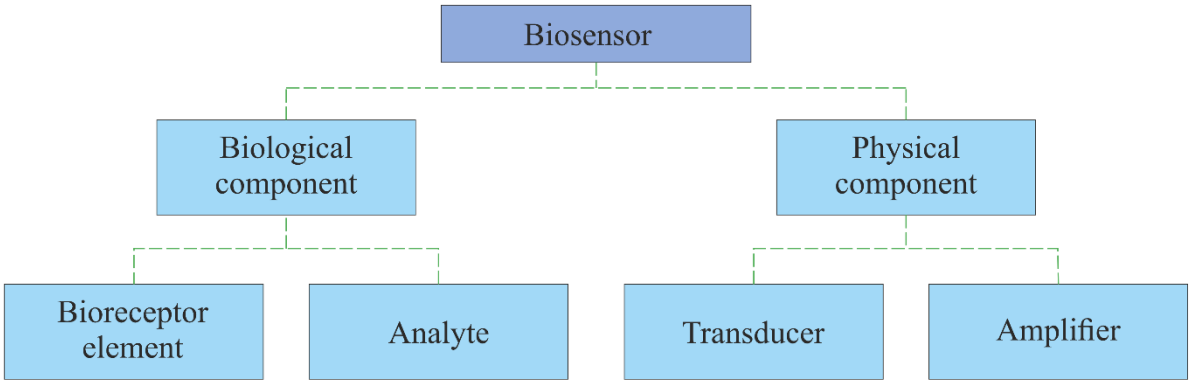

Fig. 3.1. The schematic of the components of a biosensor

Biosensors use elements for biological recognition such as enzymes, antibodies or DNA, which can attach to specific molecules called analytes, generating a biochemical interaction between the two main components, as shown in Fig. 3.1 [18-19].

Detection methods can be electrical, mechanical, or optical, measuring changes in the sample's properties due to the presence of unknown molecular species [21] .

Electrochemical impedance spectroscopy involves applying a sinusoidal voltage at different frequencies and measuring the resulting current. By varying the frequency, an impedance spectrum is obtained, which contains information about the resistance and capacitance of the interface [24] .

3.2. FIELD EFFECT BIOSENSOR

The specificity of detection, which refers to the biosensor's ability to identify and detect a single desired type of molecule, can be improved by functionalizing the sensor surface with a molecular species complementary to the unknown molecular species to be detected [27-28].

Transforming biochemical interactions into measurable signals is crucial for quantifying the concentration or presence of target molecules in a sample, using calibration curves or reference parameters for accuracy [29] .

3.3. COMPONENTS OF A BIOSENSOR

The biosensor is a device consisting of two essential and interconnected components. The receptor and the physicochemical transducer, mentioned earlier in Fig. 3.1, form the molecular recognition system.

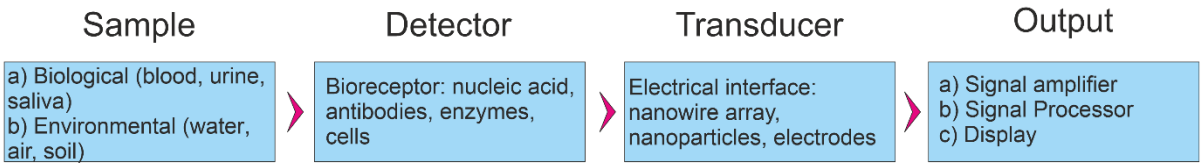

Fig. 3.2. The molecular recognition system of a biosensor [30]

The transducer converts the biochemical signal resulting from the interaction between the analyte and the bioreceptor into a measurable electrical signal, which can be used to determine the concentration or presence of the analyte in the sample, as shown in Fig. 3.2.

Signal processing in biosensors involves amplifying the signal using an amplifier and then converting it into a signal. This signal can be recorded or displayed to provide information about the concentration or presence of the detected analyte.

3.4. GENERAL CLASSIFICATION

The classification of biosensors is based on various criteria, such as the type of bioreceptor molecules or the signal transduction mechanism, as shown in Fig. 3.3.

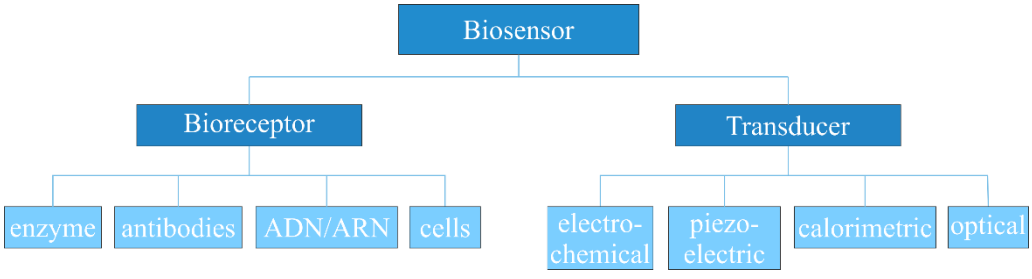

Fig. 3.3. Biosensors classification [30]

Based on the bioreceptor, biosensors are divided into catalytic biosensors and affinity biosensors.

Based on the transducer element that converts the detected signal from the physical environment into a measurable form of energy, biosensors are classified into optical, mechanical, and electrochemical biosensors.

3.4.1. Optical Biosensors

Optical biosensors utilize the optical properties of the analyte to generate luminous signals or changes in absorption, emission, or reflection of light. To obtain accurate results, rigorous calibration and proper equipment maintenance are necessary, which may involve additional costs [31] .

3.4.2. Piezoelectric Biosensors

Detection of variations in the properties of a receptor surface due to biomolecule binding can be achieved by recording the voltage or oscillation frequency of the respective surface. Using piezoelectric platforms or piezoelectric crystals as transducers in biosensors relies on the variation in oscillations generated by the deposition of a specific mass on the crystal's surface [32] .

3.4.3. Thermometric Biosensors

Thermometric biosensors measure changes in pH resulting from the release or absorption of heat produced by enzymatic processes. The amount of heat generated in an enzymatic reaction is proportional to the analyte's concentration [33] .

3.4.4. Electrochemical Biosensors

Electrochemical biosensors are the most commonly used category of biosensors. These biosensors are frequently used in applications such as DNA hybridization detection or glucose concentration determination. They combine the high sensitivity of electrochemical transducers with the specificity of biorecognition processes, generating electrical signals correlated with the analyte's concentration and enabling the monitoring of cellular processes and the determination of analyte concentration in various applications [22] .

These biosensors stand out for their simple usage, high sensitivity, and the potential for miniaturization compared to other analysis devices [31] .

3.5. ELECTROCHEMICAL DETECTION

Electrochemistry focuses on the examination of electrochemical phenomena involving the transfer of electric charge (electrons) between different chemical species. These reactions can occur at the interface between an electrode and a solution. Electrochemical biosensors utilize electrochemical species that are consumed or generated during the biochemical processes between the active biological component and the substrate immobilized on the electrode surface [34] .

Electrochemical detection measures the electrical changes generated by electrochemical reactions to determine the concentration of analytes in biological samples, using electrodes as intermediaries. This technique converts biochemical signals into electrical signals [34] .

3.5.1. Potentiometric Biosensors

Potentiometric biosensors measure the potential difference that occurs between the working electrode and the reference electrode during a redox reaction that takes place on the surface of the working electrode. These measurements are performed under equilibrium conditions, without the flow of current through the electrochemical cell. The potential measurement method is commonly used to assess the ionic concentrations at the electrode surface [35] .

3.5.2. Amperometric Biosensors

Amperometric biosensors are sensitive devices that detect and measure electroactive species present in a biological sample. These biosensors operate based on the generation of an electric current during an electrochemical reaction when a constant potential difference is applied between two electrodes. The current intensity varies depending on the oxidation or reduction reaction of the electroactive species in the analyte. An example of an amperometric biosensor is the glucose biosensor [35] .

3.5.3. Impedance Biosensors

Impedance biosensors measure the variation in the electrical resistance of a solution containing the analyte. This variation is the result of a specific biochemical reaction between the analyte and the active biological component of the biosensor. Measurements are made by applying a low-intensity alternating current signal to an electrochemical cell.

The measured impedance directly reflects this interaction and provides information about the presence and concentration of the analyte in the sample [36] .

CHAPTER 4 – THE INFLUENCE OF THE ELECTRIC FIELD ON FLUID FLOW IN MICROCHANNELS: CONTRIBUTIONS AND APPLICATIONS IN THE CONTEXT OF ELECTROCHEMICAL BIOSENSORS

4.1. APPLICATIONS OF ELECTROCHEMICAL BIOSENSORS FOR THE DETECTION AND IDENTIFICATION OF DNA HYBRIDIZATION

Electric biosensors used for studying DNA hybridization are analytical devices that utilize the principles of electrochemistry and biochemical interactions to specifically detect and measure the hybridization process of DNA single strands with complementary sequences.

DNA hybridization through the classic chain polymerization reaction occurs in three distinct stages: denaturation, hybridization, and stabilization. This step helps stabilize the double-stranded structure and subsequent DNA amplification [37] .

The use of electric field effects and microfluidics allows for controlled movement of DNA molecules, facilitating their transport and interaction with molecules immobilized on the detection surface of the biosensor [38] .

The influence of the external electric field on the transport of "target" DNA components in the double electric layer is a complex and important phenomenon in the field of electrokinetics. Helmholtz first characterized this electrokinetic transport, establishing a connection between electrical parameters and fluid movement [40] .

The Navier-Stokes law is a fundamental equation in fluid mechanics and describes the behavior of moving fluids [41] . To model fluid movement under the influence of electric fields and interactions with electrically charged particles, additional equations are needed to account for these aspects, such as those describing the concepts of electroosmosis and electrophoresis within electrokinetics [42] .

Kinetic reactions refer to the speed and rate of the biochemical processes involved in the hybridization of DNA molecules on the biosensor's surface. These include adsorption, binding, and dissociation of DNA molecules, and the reaction rate is directly proportional to the concentration of immobilized DNA molecules and those in the electrolyte [38] ,[39] .

4.2. DESIGN OF AN INTEGRATED DNA BIOSENSOR IN A MICROFLUIDIC DEVICE

Lab-On-Chip (LOC) devices represent an integrated solution that allows for the implementation of all laboratory analysis and diagnostic activities in a single miniaturized device.

In the microfluidic channel, the flow is unidirectional and laminar, ensuring the ordered movement of target molecules. The liquid is incompressible, and electroosmotic force, as well as diffusion and convection mechanisms, are essential in the movement of molecular species within the microchannel, with the reaction surface located on its lower wall, consisting of parallel plates.

In a microfluidic channel under the influence of a potential difference, there is an interaction between the electric field and the electric charges of the particles in the fluid. A double electric layer is formed near the channel wall due to the electric charges in the fluid. This phenomenon creates a potential gradient at the wall's surface, contributing to the electrokinetic transport of charged molecules in the microfluidic channel, as shown in Fig. 4.1.

The double electric layer develops a surface potential called the Zeta potential, representing the electrical tension between the dispersion medium (the liquid in which the particles are suspended) and the stationary layer of fluid in the immediate vicinity of the particles. According to studies, the average Zeta potential has a value of 25 mV for pH values ranging from 3 to 11, [41] .

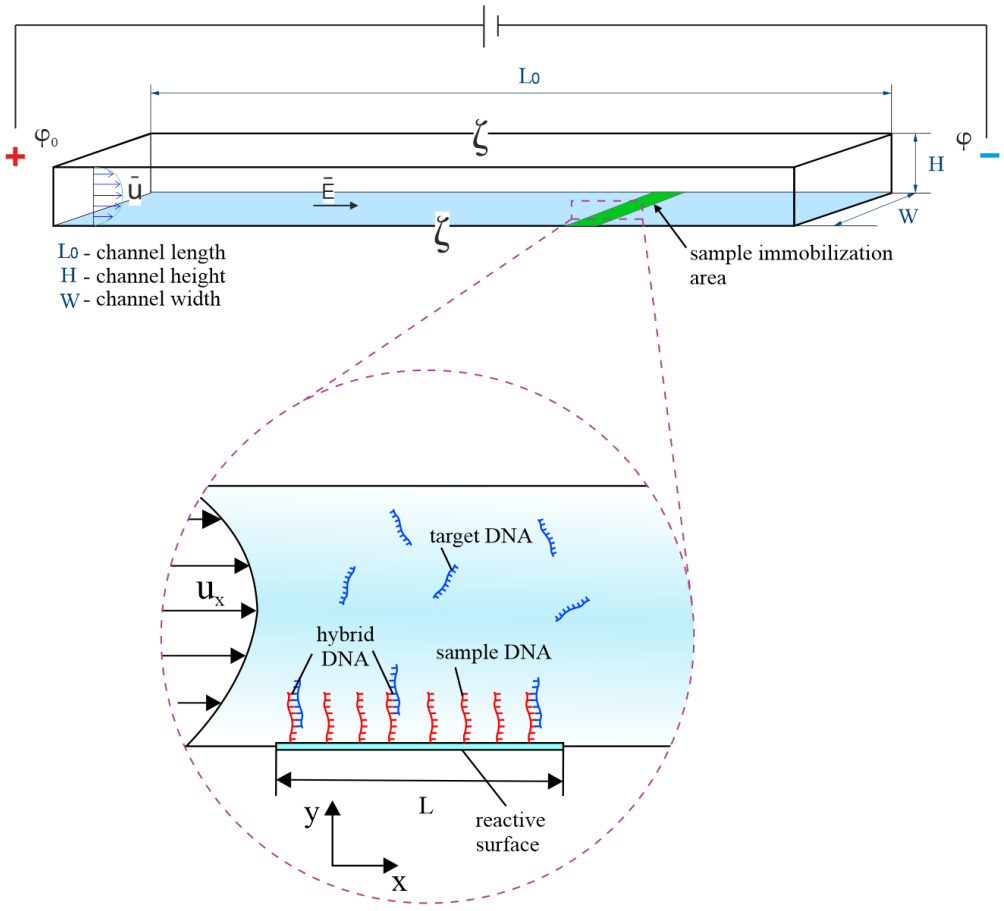

Fig. 4.1. Schematic diagram of a microfludic channel [37]

The thickness of the double electric layer, described by the Debye length, can vary from a very small scale (angstroms, which are units of measurement for subatomic lengths) to a size measured in tens or hundreds of nanometers (a nanometer representing one billionth of a meter) [43] . The value of the Debye length can be much smaller compared to the dimensions of the microchannels. In this study, the height of the microchannel varies between 25 and 50 microns [45] .

4.3. MODELING FLUID FLOW IN A MICROCHANNEL CONTROLLED BY AN ELECTRIC FIELD

4.3.1. Physical Model

The proposed *physico-mathematical model* expresses electrokinetic phenomena that occur in the flow of conducting fluids, especially in the case of heterogeneous fluids containing micrometer-sized particles or in flow over a flat surface under the influence of an electric field. Electroosmosis and electrophoresis are two distinct electrokinetic phenomena that occur in liquid systems when an electric field is applied.

The movement of the fluid and particles under the influence of the electric field is described in the physico-mathematical model using three main phenomena: fluid flow, diffusion, and electroosmosis. A static electric field applied to charged particles, such as those dispersed in a fluid, generates significant effects on their movement due to electric forces that depend on the field's magnitude and the particles' charge. This connection between particle migration and diffusion lies in the fact that particle migration can influence concentration gradients and, consequently, the diffusion process.

The problem of fluid flow in a microfluidic environment involves studying the fluid's motion in a channel or over a surface under the influence of external forces such as pressure or velocity gradient. The electrostatic problem is associated with the effect of the electric field on charged particles present in the fluid. These problems are interconnected and influence each other within the model:

1. ***In the electrostatic problem***, the application of a uniform electric field generates electroosmotic flow, causing the conductive fluid to flow in the direction of the electric field.

The Poisson equation is solved to determine the distribution of electric charges in the fluid, considering the external electric field determined by the Laplace equation. Based on this distribution and the electric potential, the mass forces of electric nature are calculated [37] .

2. ***The fluid flow problem*** describes the electrokinetic transport of charged species.

The continuity equation and *the Navier-Stokes equations* for the conservation of momentum describe laminar, incompressible, and steady fluid flow [37] .

Diffusion is a physical phenomenon in which particles, molecules or ions move from an area of high concentration to one of lower concentration according to the concentration gradient of the solution, following Fick's law [42] .

4.3.2. Mathematical Model

To analyze fluid flow in a microchannel, a two-dimensional geometry is used, considering only two spatial dimensions in accordance with the shape and physical conditions of the channel (length, height, material of the channel wall, its surface condition) [37] .

The mathematical model of an electrokinetic system involves establishing equations that describe both the *electric potential* φ, and the *concentrations of local species* c_i.

A. *External Electric Field*

In electrokinetic flow, the electric potential in a microchannel consists of two components: one generated by *the external electric field*, φ, and another caused by *the electric charges near the channel walls*, ψ [37] :

$$\Phi = \varphi + \psi \tag{4.1}$$

The driving force that determines fluid flow in a microchannel is the result of applying an external electric potential φ, which is determined by the Laplace's equation [37] :

$$\nabla \cdot (\sigma \nabla \varphi) = 0 \tag{4.2}$$

The electrostatic potential in the microchannel can be calculated using the Poisson-like equation, which expresses the relationship between the electric potential φ and the electric charge density ρ_e:

$$\nabla \cdot (\varepsilon \nabla \psi) = \frac{\rho_e}{\varepsilon_0} \tag{4.3}$$

Here, the constant dielectric ε represents the electric permittivity of the electrolyte and may vary with temperature [37] :

$$\varepsilon = 305.7 \exp\left(-\frac{T}{219}\right) \tag{4.4}$$

The total charge density is calculated using the equation:

$$\rho_e = -2n_0 ez \sinh\left(\frac{ez\psi}{k_b T}\right) \tag{4.5}$$

The ion density n_0 is expressed in molar units and is determined by the balance between positive and negative charges in the electrokinetic system [44] :

$$n_0 = \frac{\varepsilon k_b T}{8\pi e^2 z^2 \lambda^2} \tag{4.6}$$

Therefore, by including these parameters in equation (4.5), we can obtain a more detailed description of the total electric charge density in the electrokinetic system, taking into account the influence of particle valence, temperature, and geometric dimensions of the electric double layer.

B. *Flow in a Microchannel under The Influence of Pressure Gradient*

The interaction between the net charge density of the electric double layer and the applied external electric field generates a mass force that drives electroosmotic flow in the microfluidic system.

- *Mass Conservation equation* in the considered system can be written as:

$$\frac{\partial \rho}{\partial t} + (\mathbf{u} \cdot \nabla)\rho = 0 \tag{4.7}$$

- *Navier-Stokes equation* describes the conservation of momentum and can be expressed as:

$$\rho(\mathbf{u} \cdot \nabla)\mathbf{u} = -\nabla p + \nabla \cdot (\eta \nabla \mathbf{u}) + \mathbf{f}_{el} \tag{4.8}$$

where **u** [m/s] is the fluid velocity in the flow direction in the channel, ρ [kg/m^3] is fluid density, η [Pa·s] is dynamic viscosity and $\mathbf{f}_{el}$ [N/m^3] is the body force density, which is calculated as follows [38] ,[38] :

$$f_{el_x} = -\rho_e \frac{\partial \phi}{\partial x} \tag{4.9}$$

$$f_{el_x} = -\rho_e \frac{\partial \phi}{\partial y} \tag{4.10}$$

n the framework of a Newtonian fluid model, the dynamic viscosity η of the fluid depends on temperature according to the relationship [37] :

$$\eta = 2.761 \times 10^{-6} \exp\left(\frac{1713}{T}\right) \tag{4.11}$$

In this analysis, the dynamic viscosity η is considered a constant, and the temperature is fixed at a specific value of 300K. To model the components of the mass-specific force of electrical nature, boundary conditions are taken into account, which include the contribution of the external electric field and the zeta potential [37] :

$$\mathbf{u} = \frac{\varepsilon_0 \varepsilon_r \zeta_0}{\eta} \nabla \varphi \tag{4.12}$$

ζ_0 represents the Zeta potential at the channel wall, ε_0 represents the electric permittivity of vacuum and ε_r is the electric permittivity of the electrolyte, which can be expressed as a function of temperature using the relationship:

$$\varepsilon_r = 305.7 \exp\left(-\frac{T}{219}\right) \tag{4.13}$$

4.3.3. Numerical Modeling

In this work, a detailed analysis of the phenomena occurring at the channel wall-electrolyte interface is conducted using Comsol Multiphysics 5.6 software [47] .

In particular, finite element methods based on equations (4.2), (4.7), (4.8), and (4.11)-(4.13) are employed for modeling and simulating the fluid behavior within the channel and its interaction with the electrolyte, providing essential information about velocities, pressure profiles, electric charge distribution, and other relevant system characteristics.

The discretization mesh was generated with approximately 250,000 Lagrange quadratic elements [37] . The following initial conditions are imposed at the initial time ($t = 0$): the velocity in the x-direction is $\mathbf{u} = 0$, the velocity in the y-direction is $\mathbf{v} = 0$, temperature is$T = T_\infty$ and the initial concentration of DNA molecules is $c_i = 0$.

The external electric field problem, given by the Laplace equation (4.2), together with the boundary conditions mentioned in Table 4.1, which include a constant electric potential at the microchannel inlet, an electric potential of 0[V] at the microchannel outlet, and electrical insulation on the upper and lower walls of the microchannel, allows for obtaining an analytical solution, in which the electric potential is $\phi(x) = \frac{\phi_0}{L}$.

Fast system stabilization enables the swift and accurate execution of biochemical reactions and the proper guidance of particles towards detection zones [46] .

Table 4.1 is employed to establish boundary conditions, which include the following:

Table 4.1. Boundary conditions [38]

No.		Input (x=0)	Output ($x=L_0$)	Lower Wall (y=0)	Upper Wall (y=2H)
1	External Electric Field Problem (eq. 4.2)	$\varphi = \varphi_0$	$\varphi = 0$	$\frac{\partial \varphi}{\partial y} = 0$	$\frac{\partial \varphi}{\partial y} = 0$
2	Poisson-Boltzmann Electric Field Problem (eq. 4.3)	$\psi = 0$	$\frac{\partial \psi}{\partial x} = 0$	$\psi = \zeta$ *(potențial zeta)*	$\psi = \zeta$ *(potențial zeta)*
3	Flow Problem (eq. 4.7, 4.8)	$\mathbf{u} = \mathbf{u_{in}}$ **v**=0	$\frac{\partial \mathbf{u}}{\partial x} = 0$ **v**=0	**u**=0 **v**=0	**u**=0 **v**=0

Solving specific problems such as the Poisson-Boltzmann equation for the double electric layer (Eq. 4.2, 4.3) and the fluid flow analysis (Eq. 4.7, 4.8) within the system is an essential step in formulating and validating the mathematical model of microfluidic devices.

4.4. MASS TRANSFER MODELING

A. *Electroosmotic Flow in a Microchannel*

Electrokinetic flow in a microchannel, based on the theory of the electric double layer and investigated simultaneously with pressure-driven flow, can be efficiently calculated by solving the Navier-Stokes and Poisson-Boltzmann equations for the potential distribution on the channel's surface. This approach models a flow that combines the electrokinetic effect with that under pressure gradient, influenced by the electric mass forces [37] .

Energy conservation is described by the equation [46] :

$$\rho C_p \left[\frac{\partial}{\partial t} T + (\nabla \cdot \mathbf{u}) T\right] = \nabla \cdot (k \nabla T) + \varphi + \dot{q}. \tag{4.14}$$

In equation (4.14.) k represents the thermal conductivity of the electrolyte, which can be expressed as a function of temperature as follows [38] :

$$k(T) = 0.6 + 2.5 \times 10^{-5} T. \tag{4.15}$$

The heat generated as a result of electrical energy dissipation in a conductive medium can be expressed as [46] :

$$\dot{q} = \mathbf{J}^2 / \sigma. \tag{4.16}$$

where, **J** [A/m^2] represents the total electric current density.

B. ***Mass Transfer***

The species conservation equation shows that they will hybridize on the patch surface according to equations (4.2)-(4.5), [46] :

$$\frac{\partial c_i}{\partial t} + (\nabla \cdot \mathbf{u})c_i = \nabla \cdot (D_n \mathbf{J}_m) + +\mu_{os} z_i F \nabla \cdot (c_i \nabla \phi) + R_i. \quad (4.17)$$

The source term R_i is the sum of the reaction rates R_3 and R_2. These body terms shall be converted into considered boundary conditions. R_3 și R_2 represent the temporal derivatives of the specific concentrations, $c_{2,s}$ [mol] and non-specific concentrations, $c_{2,ns}$ [mol] of the target molecules adsorbed on the patch surface. The approximation of $c_{2,s}$ can be made using the linear approximation from the Taylor series [38] :

$$c_{2,s} = \frac{P}{Q}(1 - e^{-Qt}). \quad (4.18)$$

where the coefficients P and Q are calculated using the parameters k_3^1, k_3^{-1}, k_2^1, k_2^{-1} from table 4.2 and using the equations:

$$P = k_3^1 c_{3,m} \cdot c_{2,s,max} + k_2^1 c_{2,ns} \cdot c_{2,s,max}. \quad (4.19)$$

$$Q = k_3^1 c_{3,m} + k_3^{-1} + k_2^1 c_{2,ns} + k_2^{-1}. \quad (4.20)$$

Table 4.2. The kinetic constants used in numerical simulations [46]

Parameter [Unit of measurement]	**Symbol**	**Value**
The kinetic association constant for direct hybridization [1/M·s]	k_3^1	$1 \cdot 10^6$
The kinetic dissociation constant for direct hybridization [1/s]	k_3^{-1}	0.49
The kinetic association constant for indirect hybridization of non-specifically adsorbed targets [1/M·s]	k_2^1	$1 \cdot 10^6$
The kinetic dissociation constant for indirect hybridization of non-specifically adsorbed targets [1/s]	k_2^{-1}	0.51
The maximum concentration of immobilized samples on the patch surface [mol/m^2]	$c_{2,s,max}$	$2.0 \cdot 10^{-7}$
The maximum concentration of non-specifically adsorbed molecules on the patch surface [mol/m^2]	$c_{2,ns,max}$	$1.98 \cdot 10^{-7}$
The kinetic association constant for direct hybridization [1/M·s]	k_3^1	$1 \cdot 10^6$
The kinetic dissociation constant for direct hybridization [1/s]	k_3^{-1}	0.49

4.5. NUMERICAL EXPERIMENTS

The Navier-Stokes and Poisson equations describe the flow of an incompressible flow under a pressure gradient and the influence of static charge on the microchannel walls, calculated by the Poisson-Boltzmann equation. Figure 4.2 illustrates the flow field in a channel with fluid

flowing from *left to right* under the influence of a 200 V electric field and a pressure difference of 1000 Pa. Streamlines highlight the direction of fluid flow and how it reacts to the combination of the electric field and pressure gradient [46] .

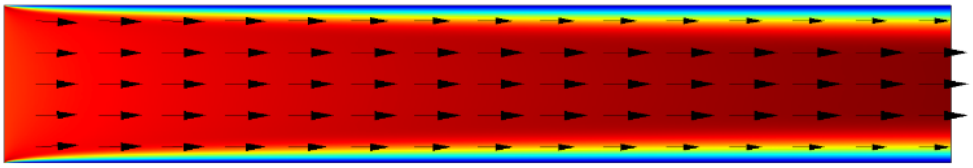

Fig. 4.2. The fluid flow for H/L = ($5 \cdot 10^{-4}$ m) / ($3 \cdot 10^{-3}$ m),
Δp = 1000 Pa (from left to right), V = 200 V (from left to right) [37] .

Figure 4.3 shows the flow profile in the channel under different pressure drops while keeping the other conditions unchanged. It can be observed that the flow profile in the channel follows the Hagen-Poiseuille model [38] , which describes laminar flow of a fluid in a channel. The velocity profile is presented 2.5 mm inside the flow channel. Here, the velocity profile is stable and well-defined, with an aspect ratio (AR) of 0.12, indicating a uniform distribution of velocities in the channel with no significant variations.

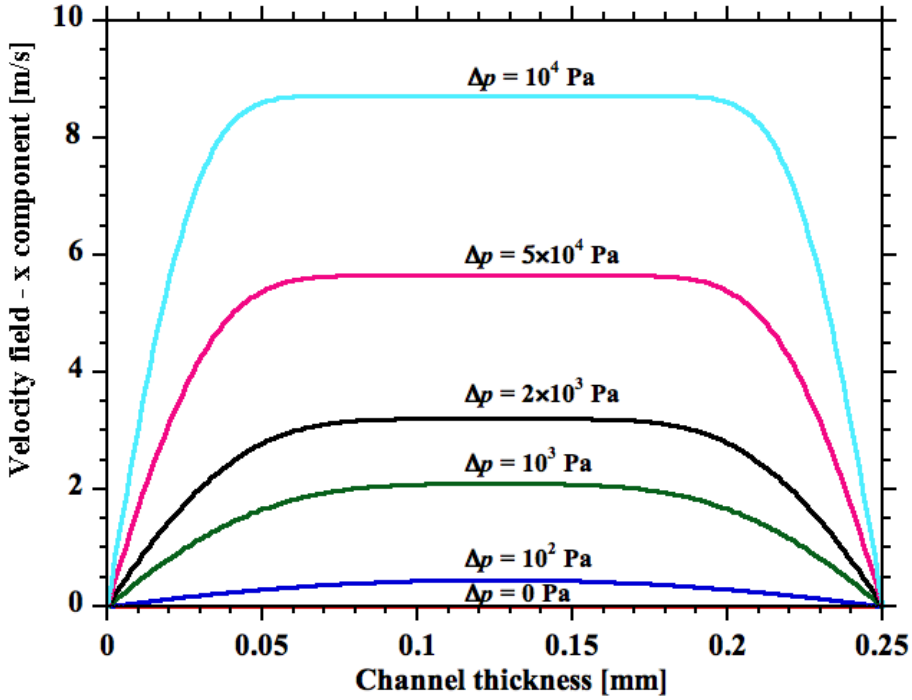

Fig. 4.3. The velocity profile for increasing Δp at x = 2.5 mm (along the flow),
in the fully formed region has an aspect ratio (AR) of 0.12 [37]

In Fig. 4.4, velocity profiles in the same channel are presented, considering two simultaneous influences: the pressure difference from *right to left* and the *unchanged direction of the electric field from left to right*. This provides a comparison of how these two factors affect the velocity distribution in the channel.

In this case, the direction of fluid flow has reversed compared to the first case due to the pressure difference acting in the *right-to-left direction*, causing fluid movement from *right to left*. Thus, both the electric field and the pressure difference contribute to fluid flow in the opposite direction.

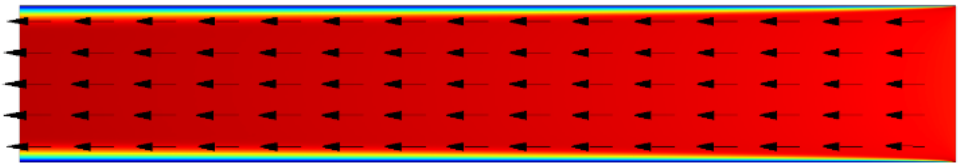

Fig. 4.4. The fluid flow for H/L = (5·10^{-4} m) / (3·10^{-3} m),
$\Delta p = 1000\ Pa$ (from right to left), V = 200 V (from left to right) [37]

In Fig. 4.5, velocity profiles in the same channel are examined under conditions where different pressure differences act from *right to left*, while the direction of the electric field remains from *left to right*.

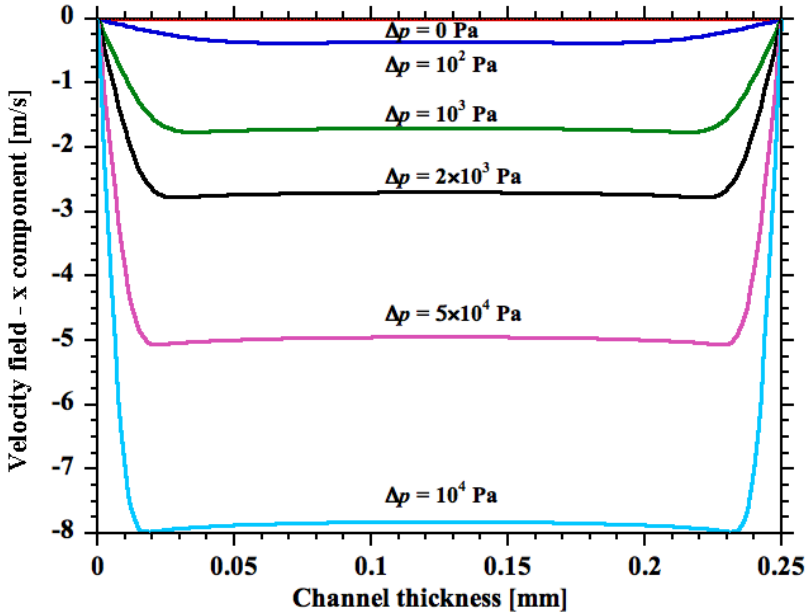

Fig. 4.5. The velocity profiles for increasing Δp at x = 2.5 mm (along the length), in the fully formed region for (AR) of 0.04;
V = 150…200 V (from left to right) [37]

Comparing the color map in Fig. 4.4, which shows flow from *right to left* while maintaining the direction of the electric field from *left to right*, with the color map in Fig. 4.2, which indicates flow from *left to right*, we observe a general reversal in the direction of fluid flow in the two cases. However, the *direction of the electric field remains constant*, from *left to right*, in both situations [37] .

The numerical results have confirmed agreement with literature data, for example [44] and have highlighted the importance of the regions adjacent to the walls in electroosmotic flow.

The velocity profiles were consistent with Hagen-Poiseuille theory in channels, and pressures and velocities were similar to experimental data.

The concentrations of the two types of hybridization, specific and nonspecific, stabilize over time due to reaching an equilibrium between the processes of association and dissociation, where the rates of these processes gradually become equal. This equilibrium leads to the stabilization of concentrations, indicating that the system has reached an equilibrium point [46]. Specific and nonspecific hybridization were analyzed through kinetic studie [38], especially in the context of the "exhaustion" of target molecules at the patch surface. The two mechanisms of specific and nonspecific hybridization are highlighted in Fig. 4.6 at the patch surface [46].

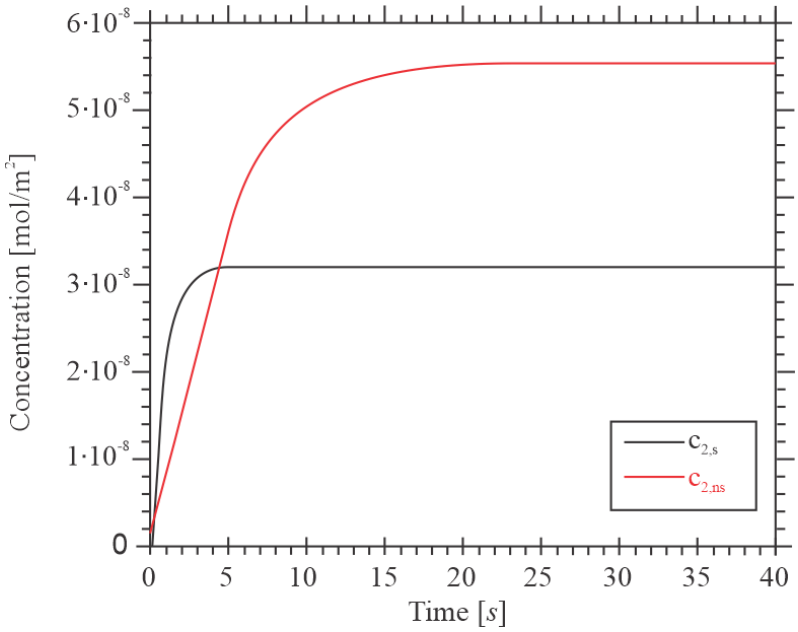

Fig. 4.6. Concentrations of specific and nonspecific target molecules adsorbed at the patch surface [46]

4.6. CONCLUDING REMARKS DERIVED FROM THE SIMULATIONS

This study has generated substantial insights into the domain of DNA hybridization within a microchannel and the management of this process through the application of electric fields and control over fluid flow rates. The investigation has probed the impact of these factors on the efficiency of DNA hybridization.

The computational simulations conducted in this study have revealed important findings regarding the dynamic behaviors of fluids within lab-on-chip devices in response to pressure gradients and electric fields. The hybridization process exhibits notable efficiency and rapidity, with concentrations stabilizing promptly. These outcomes collectively suggest a highly advantageous process within the microfluidic system.

CHAPTER 5 - CHARACTERIZATION OF ELECTRICAL PROPERTIES OF 3D PRINTED ELECTRODES: CONTRIBUTIONS TO THE DEVELOPMENT OF ELECTROCHEMICAL BIOSENSORS

5.1. DESIGN AND FABRICATION OF 3D PRINTED ELECTRODES

Electrochemical biosensors are advanced tools for the detection and monitoring of analytes of biological or environmental significance. In recent years, biosensors have gained increasing importance in the field of clinical diagnostics, particularly for the detection of infectious diseases and health monitoring [48] .

The fabrication of electrodes traditionally relies on conventional techniques such as screen printing and photolithography, which involve labor-intensive work, require processing in a controlled environment with high levels of cleanliness and purity, and involve multiple steps using toxic materials [50] .

In the 3D printing of electrodes, several specific techniques are used for electrode creation, including extrusion-based printing, inkjet-based printing, and laser-assisted printing [58] .

5.1.1. Designing Electrode Geometry

The development of 3D printing technologies has enabled the creation of electrodes with customized geometries and improved performance, enhancing the detection capabilities and analytical precision of biosensors [56] .

Electrodes with a larger perimeter exhibit a significant increase in the interaction area with analytes, thus increasing the chances of capturing a greater number of molecules in a short period, such as biosensors used for rapid detection of bacterial infections in blood samples. This is due to the electric field generated by the electrodes, which extends into the vicinity of the perimeter and influences the surrounding area.

Various configurations of working electrodes are created, encompassing a wide range of shapes, geometries and different dimensions: circular shape, square shape, gear shape, star shape, S-shape, Fibonacci shape [57] .

5.1.2. Manufacturing Method

Several 3D printing techniques can be used for electrodes, namely extrusion-based printing, inkjet-based printing, and laser-assisted printing. The manufacturing process used for making the electrodes is presented in [59] .

a. Substrate

For electrode fabrication, a 50 μm-thick adhesive polyimide film (Kapton®) [59] was used. To ensure the application of the Kapton film without air bubbles or wrinkles, a flat and uniform surface is required as a solid support [60] .

b. Carbon-Based Ink

Carbon-based ink is an excellent electrical conductor, maintains its shape and adhesion during 3D printing, and is biocompatible, making it suitable for use in contact with the body without the risk of adverse reactions [60] .

c. Printing Parameters

Extrusion pressure (p) determines the force applied to the material during the extrusion process. *Printing speed* refers to the speed at which the print head moves during material deposition. *Layer height* refers to the thickness of each printed layer in the extrusion process.

d. Generating G-code File

The process of designing electrode configurations is carried out through computer-aided design (CAD) software, which generates 3D models of the electrodes.

e. Post-processing

To enhance the conductivity and stability of the printed electrodes, a uniform heat treatment is applied at 140°C for 30 minutes, removing moisture and consolidating the material while improving its conducting properties.

f. Surface Functionalization of the Electrode. Immobilization of Antibodies

Biological receptors can be immobilized on the surface of the transducer using various procedures, including immobilization behind a permeable membrane for analytes, in a polymeric matrix, in monolayers or lipid membranes, direct adsorption, covalent binding, or cross-linking [62]

5.2. CHARACTERIZATION OF ELECTRICAL PARAMETERS USING ELECTRIC IMPEDANCE SPECTROSCOPY

5.2.1. Device Setup

A potentiostat is a device used in electrochemistry to control and monitor electrochemical processes occurring on the surface of electrodes. It allows for the controlled application of a potential between electrodes and the measurement of the resulting current during electrochemical reactions.

In the experiment, six different shapes of printed electrodes were tested, as shown in Fig. 5.1. The purpose of this experiment was to determine the optimal electrical parameters for each electrode configuration. The electrical pathways and the electrode surfaces were created using carbon-based ink, characterized by good electrical conductivity that ensures efficient electrical current transfer between the electrodes.

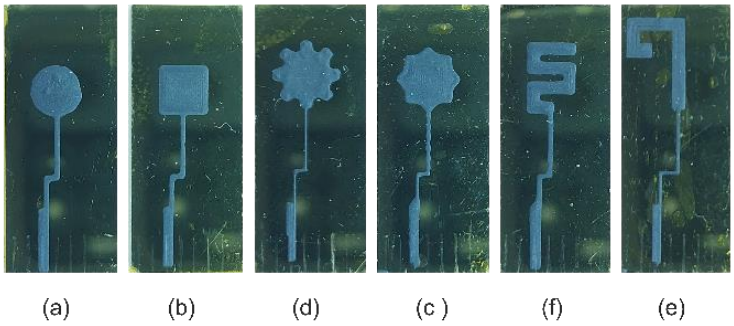

Fig. 5.1. Configurations of the working electrodes: a) Circle; b) Square; c) Gear; d) Star; e) "S" shape; f) Fibonacci [54] .

Figure 5.2 depicts a 3-electrode configuration used in the experiment: a 3D-printed working electrode (WE), a Metrohm LL-Ag/AgCl standard reference electrode (RE), and an auxiliary electrode (CE) made from a thin platinum foil. This configuration enables precise control and measurement of the working electrode's potential in relation to the reference electrode, while the auxiliary electrode consistently provides electrons to support the electrochemical reaction.

Fig. 5.2. Support for the 3-electrode cell: a) 3D-printed Working Electrode (WE); b) Redox solution; c) Auxiliary/Counter Electrode (CE); d) Reference Electrode (RE) [54] .

5.2.2. Experimental Conditions for Characterizing 3D-Printed Electrodes

The experiments were conducted on 3D-printed working electrodes placed in an electrolyte containing potassium ferrocyanide (K4[Fe(CN)6]). This compound served as the analyte, allowing electrochemical reactions to occur on the electrode's surface and generating a measurable electric current in this electrochemical medium.

When evaluating the electrochemical behavior of a system in a particular reactive medium, temperature plays a significant role as electrochemical properties can vary with it [54] .

5.2.3. Electrical Measurements

Cyclic voltammetry provides information about the behavior of electrodes as a function of applied potential, including oxidation and reduction potentials, electron transfer rates, and surface characteristics. Electrochemical impedance spectroscopy (EIS) measures the electrochemical response at different frequencies [54] .

Parameters measured in electrochemical impedance spectroscopy (EIS) include the magnitude and phase of impedance, which reflect the resistive or capacitive nature of the electrochemical system. Additionally, the real and imaginary components of impedance can be determined, indicating specific properties of the electrode-electrolyte interface, such as charge transfer resistance, double-layer capacitance, and Warburg impedance, which reflects the diffusion of ions in solution.

Warburg impedance is a circuit element associated with the diffusion process of electroactive species and their movement toward the surface of an electrode [66] .

5.3. EXPERIMENTAL RESULTS

Electrochemical impedance spectroscopy (EIS) was employed to investigate the influence of the working electrode geometry on the performance of three-electrode biosensors.

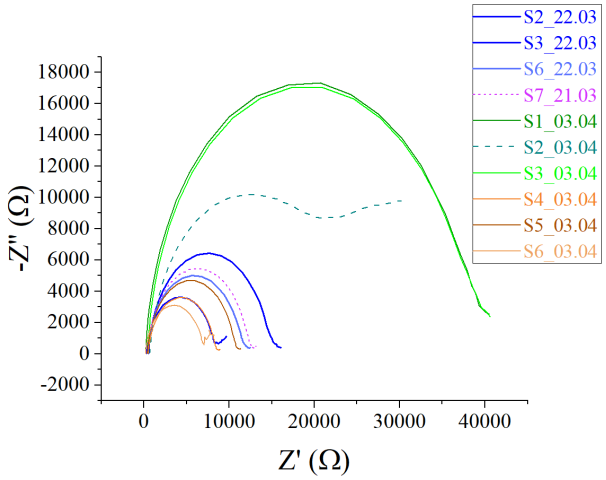

Fig. 5.3. Plot of the Nyquist diagram for the impedance response – Table 5.1

The experiments covered a frequency range from 0.1 Hz to 100 kHz, and the electrochemical data were recorded through a connection between the working electrode, electrolyte, and a potentiostat. The impedance response was investigated using potassium ferrocyanide as the electrolyte. Six different active surfaces of the working electrodes were tested to analyze the effect of varying their active area. The impedance response was analyzed through a Nyquist plot, as shown in Fig. 5.3. The plot reveals the competition between surface and bulk diffusion processes coupled with charge transfer processes [61 , 64] .

The phase angle is the phase difference between two signals or waveforms. It can be expressed in degrees or radians and reflects the phase difference of a signal or waveform compared

to a reference signal or waveform. In the case of electrochemical biosensors, the phase angle can indicate changes in the interactions between the analyte and the bioreceptor immobilized on the electrode surfaces [67] .

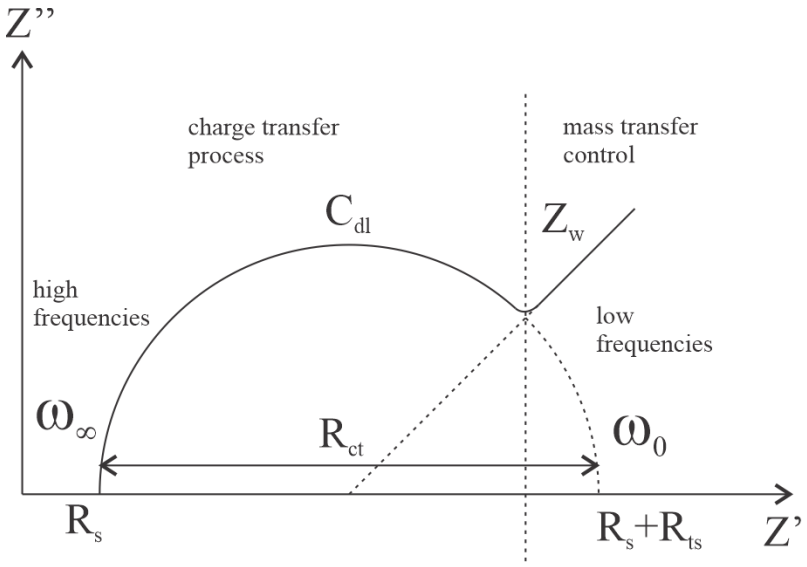

Fig. 5.4. Representation of Nyquist diagram

In each configuration, the electrochemical parameters were determined. The charge transfer resistance (Rct) results from the transfer of electrons between the electrode and the solution. The charge transfer resistance, represented in the Nyquist diagram in Fig. 5.4, as indicated by the diameter of the semicircle, appears in the low-frequency region and is used to evaluate the efficiency of the electron transfer process at the electrode-electrolyte interface [67] .

Constant Phase Elements (CPEs) are mathematical models used to describe the non-ideal behavior of electrode surfaces in electrochemistry. They are represented by the terms Q and n, where Q is the constant phase element and n is the phase exponent.

The impedance of the constant phase element Z_{CPE}, is given by the equation [65] :

$$Q = Z_{CPE(\omega)} = [C(j\omega)^n]^{-1} \quad (5.1.)$$

where j is an imaginary number and ω [rad·s-1] is the angular frequency.

Polarization resistance, R_p represents the opposition of the electrochemical system to voltage variation, reflecting how efficiently the system responds to these changes.

The maximum imaginary impedance (Z''_{max}) is an important component of electrochemical impedance, indicating the point at which energy storage capacities are maximum at a specific frequency.

Double-layer capacitance, C_{dl}, represents the capacity to store electric charge at the interface between the electrode and the electrolyte [67] .

Table 5.1 Electrical Properties of Working Electrodes

	φmax	**Z"max [Ω]**	**Rct [Ω]**	**Rp [Ω]**	**Cdl [mF]**	**Y0 [CPE]**	**N**
S1_03.04 Circle	77.48	17308	20660	40474	3.07	1.51E-06	0.94

S3_03.04 Circle	73.65	17035	17279	40600	2.91	1.51E-06	0.94
S2_03.04 Circle	64.30	10189	11933	20722	6.69	3.61E-06	0.91
S2_22.03 Fibonacci	63.62	6434	7677	15451	2.61	1.40E-06	0.94
S7_21.03 Gear	64.68	5460	6453	13020	1.96	1.04E-06	0.95
S5_03.04 Square	62.90	4670	6027	11187	1.67	8.77E-07	0.95
S6_22.03 Star	63.06	5014	5658	12400	2.81	1.53E-06	0.94
S3_22.03 S-Form	63.88	3609	4434	8457	1.80	9.57E-07	0.93
S4_03.04 Square	57.52	3573	4014	8760	1.58	9.13E-07	0.95
S6_03.04 Square	65.13	3118	3579	7056	1.77	9.50E-07	0.96

Based on the data obtained from the Nyquist plot, an equivalent circuit model for a biosensor is created, as shown in Figure 5.5 [54] .

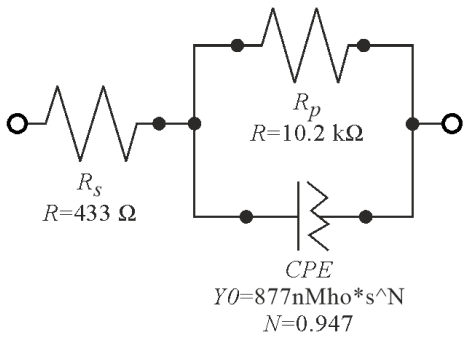

Fig. 5.5. The Randles circuit for the electrode S5_03.04.2023 [54]

The relationship between current intensity and applied voltage for the 10 tested working electrodes is illustrated in Fig. 5.6 in a cyclic voltammetry plot. It can be observed that both oxidation and reduction peaks appear in the cyclic voltammogram.

The phase difference (φ), the admittance of the constant phase element YCPE and the number N are quantities that reflect the electrochemical behavior of the system (as presented in Table 5.1) and are influenced by changes in system parameters. Cyclic voltammetry (CV) measurements were conducted using a range of potentials from -0.4 V to 0.4 V and a scan rate of 100 mV/s.

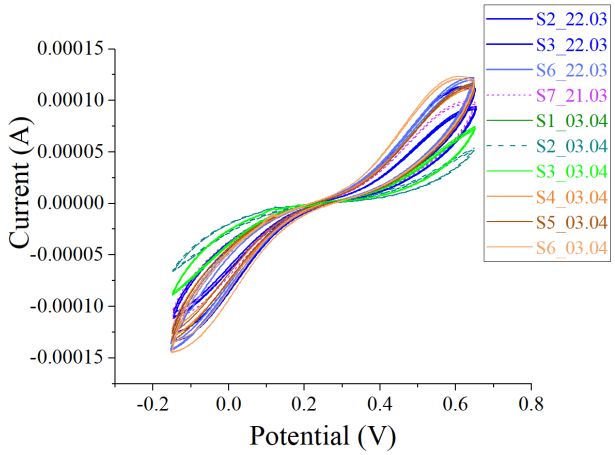

Fig. 5.6. The cyclic voltammetry plot for the sensors listed in Table 5.2 [54]

According to the experimental results, circular-shaped electrodes recorded the highest values of charge transfer resistance (R_{ct}), as shown in Fig. 5.7, indicating a slower charge transfer compared to square-shaped electrodes, which exhibited the lowest (R_{ct}) values.

This slowing down of charge transfer can affect the detection capability and response to variations in specific properties such as temperature, analyte concentration, and the pH of the electrolyte solution. To detect under such conditions, higher potentials or longer measurement times may be required.

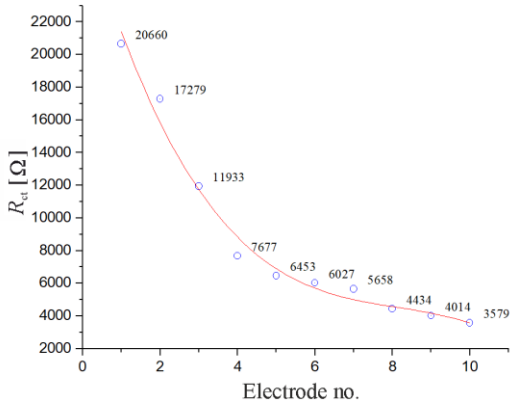

Fig. 5.7. The R_{ct} variation graph for the sensors listed in Table 5.1 [54]

Cyclic voltammetry measurements generate distinct peaks in the recorded current graph, representing specific electrochemical processes such as oxidation and reduction of chemical species at the electrodes. The peak height represents the maximum current value recorded during these electrochemical reactions, thereby reflecting the intensity and significance of these processes [65] .

Analyzing the data from Table 5.2 indicates that geometries with a larger perimeter have lower charge transfer resistance and a higher maximum current compared to those with a smaller perimeter. This suggests that perimeter is a crucial factor in determining the electrochemical performance of the system.

Table 5.2 Surface, area, perimeter and maximum current of WE as a function of geometry

Electrode Name	Area [mm^2]	Perimeter [mm]	Peak i_a [A]
S6_22.03_Star	18.7	18.746	4.3347E-05
S3_22.03_S-Shape	10.5	36.4	3.8249E-05
S2_22.03_Fibb	12.8	33.8	3.5004E-05
S5_03.04_Square	16	16	3.4988E-05
S4_03.04_Square	16	16	3.4847E-05
S7_21.03_Gear	16.4	25.462	3.4625E-05
S6_03.01_Square	16	16	2.5894E-05
S3_03.04_Circle	12.5	12.566	5.6728E-06
S1_03.04_Circle	12.5	12.566	5.5674E-06
S2_03.04_Circle	12.5	12.566	4.2851E-06

5.4. CONCLUSIONS

This study focuses on characterizing the electrical properties of 3D-printed biosensors, with a strong focus on various configurations of working electrodes. Using techniques such as electrochemical impedance spectroscopy and cyclic voltammetry, we investigated the influence of geometric characteristics on the electrochemical performance of these electrodes. By simplifying the manufacturing process through the printing of only the working electrodes and associated electrical traces, we reduced costs and used resources more efficiently. The working electrodes are responsible for electrochemical reactions and generating electric current in electrochemical processes, while the electrical traces provide the connection between the electrodes and the potentiostat.

The shape of the electrodes has a significant impact on the distribution of the electric field and interaction with the analyte. Complex shapes such as gearwheels or the Fibonacci shape can create non-uniform electric field distributions, while simple shapes like circles or squares favor a uniform distribution. These differences in electric field distribution can influence how the analyte interacts with the electrode surface, affecting the efficiency of analyte detection.

The 3D printing process introduces variations in the porosity and composition of the electrodes. Carbon paste density, thickness of the active layer, uniformity of paste deposition, and electrode attachment method all impact the electrochemical response. Measurement errors can arise for various reasons, and recognizing and accounting for these sources of error in the experiment are important for gaining a comprehensive understanding of the results [54] .

In conclusion, the design of square-shaped electrodes offers clear advantages in terms of electrochemical performance, particularly in terms of the charge transfer resistance (R_{ct}). Square-shaped electrodes provide more efficient charge transfer between electrodes and the analyte solution, improving biosensor performance.

CHAPTER 6 – CONCLUSIONS AND PERSPECTIVES

6.1. CONCLUSIONS

In recent years, the concept of lab-on-a-chip, initially developed in the academic environment, has seen remarkable evolution and has been successfully implemented in commercial products.

This PHD Thesis focuses on analyzing how advanced electromagnetic methods are applied in biomedical research, with a special attention given to the development of electromagnetic biosensors used for detecting biochemical particles. The primary goal of the thesis was to study the interactions between the electromagnetic field and the biological environment for the detection and analysis of biochemical particles.

The research was oriented towards two main areas of analysis: modeling the effects of applying an electric field on fluid flow in microfluidic structures and designing and manufacturing electrodes used in electrochemical biosensor manufacturing.

Modeling the interactions between electromagnetic fields and fluid behavior in microfluidic structures revealed complex phenomena and subtle interactions that are difficult to observe experimentally. This approach significantly contributed to understanding the physical processes within biosensors integrated into microfluidic platforms, such as fluid movement in microchannels, molecule transport, and biomolecule interactions with the functional surfaces of microfluidic devices in the context of electrochemical reactions.

By designing and manufacturing electrodes for electrochemical biosensors used in detecting ion concentrations in a solution, electrodes with precise geometries adapted to specific experimental requirements of electrochemical biosensors were obtained.

6.2. ACHIEVING RESEARCH OBJECTIVES

In Chapter 1, an introduction to the thesis topic is provided, presenting basic concepts related to the use of electromagnetic methods in biomedical process research.

Chapter 2 focuses on analyzing the current state of research in biosensors, their integration into microfluidic platforms, and the evolution of 3D printing technology for creating advanced electrodes.

Chapter 3 presents the issues related to biosensors, with special attention to aspects concerning their classification, structure, and operation. Electrical detection methods are presented as a central component of biosensors, highlighting how they transform biochemical interactions into measurable electrical signals.

Chapter 4 is dedicated to physico-mathematical modeling and the analysis of complex interactions and couplings between the electromagnetic field, fluid flow, and electrically charged particles in a microfluidic environment, emphasizing the influence of the electric field on electroosmosis and other phenomena.

The main results of this study include identifying the impact of the electric field on pressure-driven flow, observing velocity profiles based on pressure variation, highlighting the importance of regions adjacent to channel walls, validating the effectiveness of the hybridization process, and confirming the results through comparison with relevant experimental data from the literature.

Chapter 5 analyzed the potential of impedance spectroscopy as a research method for identifying biochemical compounds. This method provides significant data on the behavior of various biomolecules in a system by monitoring the variation of specific physical parameters of the system's components.

6.3. PERSONAL CONTRIBUTIONS

We analyzed the electric field generated by electric charges close to the channel walls, known as the electric double-layer potential, which occurs at the interface between the channel wall and the electrolyte. We determined how this electric field, applied along the channel, interacts

with electric charge density. On the other hand, this interaction generates the appearance of electric forces that drive electroosmotic flow in the microfluidic system.

Another important aspect of the research focuses on modeling mass transfer in a microchannel with electroosmotic flow. This study combines electrokinetic flow, based on the electric double-layer theory, with pressure-driven flow in a microchannel, using the Navier-Stokes equations and the Poisson-Boltzmann equations to analyze subtle phenomena and complex interactions that cannot be easily observed experimentally.

It was observed that applying an electromagnetic field can influence the variation of the double-layer properties, which, in turn, affects the interactions between the particles in the electrolyte and the electrode's functional surfaces. These modifications can have a significant impact on particle behavior, opening the possibility of selectively controlling their movement and capture in various zones of microchannels.

Within the research, the thermal equilibrium of the system was also analyzed using the heat equation. It was found that the heat sources generated by viscosity and Joule heating are small enough to maintain the system at a constant temperature of 300 K.

The numerical studies conducted have provided an improved perspective on the mechanisms underlying fluid behavior and transport processes in microscopic environments.

Significant practical contributions have been made through the optimization of the electrode manufacturing process for electrochemical biosensors, using 3D printing technology with carbon-based materials. This approach allowed for obtaining electrodes with precise "geometries" tailored to the specific experimental requirements of biosensors.

The characterization of the electrochemical properties of the electrodes was achieved through electrochemical impedance spectroscopy (EIS), a technique that provides detailed information about the behavior of electrodes in interaction with the biological environment or analytes.

6.4. RESULTS DISSEMINATION

The research results have been disseminated through the publication of three scientific papers. Two of these papers were presented at the ATEEE conference. The third paper was published in RRST-EE (Revue Roumaine des Sciences Techniques, Sèrie Électrotechnique et Énergétique), a recognized journal with broad visibility in the academic community.

By combining knowledge from electrical engineering applied to microfluidic technologies and biomedical research, an innovative perspective has emerged in the field of molecular detection and analysis. On the one hand, electrical engineering has brought to the forefront methods that enable fluid manipulation at the micrometer scale under the influence of an external electric field. Future research may integrate mathematical simulation to complement experimental studies obtained in practice regarding 3D-printed electrodes, offering a more comprehensive understanding of electrode behavior and their potential in various applications.

GLOSSARY OF SPECIFIC TERMS

1. Adsorption - the process by which molecules, ions, or atoms adhere to and accumulate on the surface of a solid or liquid material. This occurs when chemical species from the surrounding environment (called adsorbates) bind or "stick" to the surface of the material (called the adsorbent) through intermolecular forces.
2. Lipid Bilayer - a structure consisting of two layers of lipid molecules, with polar heads oriented outward and nonpolar tails oriented inward. This structure is essential in biology and medicine, providing a physical and chemical barrier between the cell's internal and external environments.
3. Ionic Channel - a special type of protein that forms pores or channels in cell membranes. These channels allow ions to pass through the membrane and are selective for specific ions, regulated by various factors such as voltage changes or ion concentration in the environment.
4. Active Channels - a type of ion channel that requires energy to function and allows the passage of ions through the membrane. This type of channel is controlled and regulated by the cell and can be opened or closed depending on different signals or stimuli.
5. Passive Channels - a type of ion channel that allows the passage of ions through the membrane passively, without requiring energy consumption by the cell. This type of channel opens and closes depending on the differences in electric potential or ion concentration in the surrounding environment, allowing ions to pass in a manner determined by external conditions.
6. Double-Stranded Complex - a molecular structure formed by two complementary chains of nucleic acids (DNA/RNA) that attach to each other through complementary base pairing.
7. Electroosmotic Flow - an electrochemical phenomenon that occurs in microfluidic or capillary systems. It is generated by applying an electric field to a conductive fluid in a microchannel, inducing a net flow of liquid that moves in the opposite direction of ion migration.
8. Desorption - the opposite process of adsorption, referring to the release of adsorbates (molecules, ions, or atoms) from the surface of the adsorbent. During desorption, the chemical species that have attached or been adsorbed to the adsorbent's surface are released back into the environment. This process can be triggered by changing external conditions, such as temperature, pressure, or the concentration of the adsorbate substance.
9. Hybridization - the process of pairing two complementary nucleic acid molecules (DNA or RNA) to form a structure known as a double helix or double-stranded complex. During hybridization, the nitrogenous bases on the two strands bind together through complementary base pairs (adenine with thymine in DNA or adenine with uracil in RNA, and guanine with cytosine), forming strong chemical bonds.
10. Extracellular Environment - the space surrounding living cells, which separates them from the external environment.
11. Intracellular Environment - the space inside the cell.

12. Cell Membrane - a fundamental structure of living cells that delineates the cellular contents from the external extracellular environment. It is a thin, flexible, and elastic membrane composed of a double lipid bilayer and proteins, serving various essential functions in cellular life.
13. Microarray - an analytical device used to detect and quantify the presence and quantity of specific biological molecules, such as DNA, RNA, proteins, or other biological molecules, in a biological sample. This device consists of a solid surface (usually a glass or silicon wafer) on which thousands or even millions of microprobes are fixed in a controlled and ordered manner. These microprobes contain specific DNA or RNA sequences, known as probes, designed to search for specific molecules in the analyzed sample.
14. Single-Stranded Molecule - a single chain of nucleic acids (DNA/RNA) that is not associated with a complementary second chain through base pairing.
15. Sequencing - a complex and essential process in molecular biology that involves determining the precise order of nucleotide bases (adenine, thymine, cytosine, and guanine) in a molecule of nucleic acids (DNA or RNA). This process includes reading and recording the nucleotide sequence in a single-stranded DNA or RNA molecule, allowing for the exact identification of the sequence.
16. Conformational State - a specific configuration or structure in which a molecule, protein, or another type of macromolecule exists, depending on the interactions and bonds between its atoms and functional groups.
17. Proteins - complex molecules essential for life, consisting of chains of amino acids connected in unique sequences. They represent one of the most diverse and important classes of macromolecules in living organisms.
18. Hybridization Rate - the speed at which single-stranded DNA/RNA molecules form complementary base pairs with each other to create a double-stranded structure of nucleic acids. This rate measures how quickly the binding process occurs between single-stranded molecules with their complementary sequences.
19. Cellular Transport - refers to the movement of substances into and out of cells within living organisms. There are two main types: passive transport and active transport.

References:

[1] Ramos, A., & Suzuki, D. O. H., "*Computational Approach for Electrical Analysis of Biological Tissue Using the Equivalent Circuit Model*", Handbook of Electroporation, 1–21, 2016, DOI:10.1007/978-3-319-26779-1_12-1.

[2] Y. Liu, "*Mathematical and Computational Modelling for Biosensors: a Modular Approach. Doctoral Thesis*". Technological University Dublin, 2012, DOI:10.21427/D7XS3N.

[3] S. Gogoneata, "*Biosenzor electrochimic pentru detectia hibridizarii AND-ului*", Teza de Disertatie, Universitatea Politehnica Bucuresti, Facultatea de Inginerie Medicala, 2020.

[4] S. Radke, E. Alocilja, "*Design and fabrication of a microimpedance biosensor for bacterial detection*", IEEE Sens. J. 2004, 4, 434–440.

[5] J. Chen, Z. Fang, J. Liu, L.A. Zeng, "*A simple and rapid biosensor for ochratoxin based on a structure-switching signaling aptamer*". Food Control 2012, 25, 555–560.

[6] X. Zeng, Z. Shen, R. Mernaugh, "*Recombinant antibodies and their use in biosensors*", Anal. Bioanal. Chem. 2012, 402, 3027–3038.

[7] C. Savran, S. Knudsen, "*Micromechanical detection of proteins using aptamer-based receptor molecules*", Anal. Chem. 2004, 76, 3194–3198.

[8] N.S. Mazlan et all., "*Interdigitated electrodes as impedance and capacitance biosensors: A review*", AIP Conference Proceedings 1885, 020276 (2017), DOI: 10.1063/1.5002470.

[9] J.C. Vanegas Acosta, "*Electric fields and biological cells : numerical insight into possible interaction mechanisms*", Technische Universiteit Eindhoven, 2015.

[10] A. Yúfera, G. Huertas, and A. Olmo. "*A Microscopy Technique based on Bio-impedance Sensors*" Procedia Engineering, vol. 47, 2012. DOI:10.1016/j.proeng.2012.09.330

[11] E. Sieni, "*Biomedical Applications of Electromagnetic Fields: Human Exposure, Hyperthermia and Cellular Stimulation*", University of Padova, 2011.

[12] R. Bansal, "*Handbook of Engineering Electromagnetics*", University of Connecticut, 2004

[13] Q. Wang, "*Mathematical Methods for Biosensor Models. Doctoral Thesis*", Technological University Dublin, 2011. DOI:10.21427/D7BS3C.

[14] S. K. Mitra, S. Chakraborty, "*Microfluidics and Nanofluidics Handbook. Fabrication, Implementation and Application*", Taylor & Francis Group, 2012.

[15] Manocha, Puneet & Chandwani, Gitanjali & Das, Soumen. (2020). "*Characterization of Dielectrophoresis Based Relay Assisted Molecular Communication Using Analogue Transmission Line*". IEEE Access. PP. 1-1. 10.1109/ACCESS.2020.2974067.

[16] Ahmed, Riaz, and Reifsnider, Kenneth L. "*Study of Influence of Electrode Geometry on Impedance Spectroscopy*". United States: N. p., 2011. Web. doi:10.1115/FuelCell2010-33209.

[17] Wang, Z.; Murphy, A.; O'Riordan, A.; O'Connell, I. "*Equivalent Impedance Models for Electrochemical Nanosensor-Based Integrated System Design*". Sensors 2021, *21*, 3259. https://doi.org/10.3390/s21093259.

[18] Conroy P. J., Hearty S., Leonard P. & O'Kennedy R. J., "*Antibody production, design and use for biosensor-based applications*", Seminars in Cell & Developmental Biology (2009), 20(1), 10–26. doi:10.1016/j.semcdb.2009.01.010

[19] Yang X., Qian J., Jiang L., Yan Y., Wang K., Liu Q. & Wang K., "*Ultrasensitive electrochemical aptasensor for ochratoxin A based on two-level cascaded signal amplification strategy*", Bioelectrochemistry (2014), 96, 7–13. doi:10.1016/j.bioelechem.2013.11.006

[20] Suehiro J., Yatsunami R., Hamada R. and Hara M., "*Quantitative estimation of biological cell concentration suspended in aqueous medium by using dielectrophoretic impedance measurement method*", Journal of Physics D: Applied Physics, 32(21), 2814–2820. doi:10.1088/0022-3727/32/21/31.

[21] Zheng D., Zou R. & Lou X., "*Label-Free Fluorescent Detection of Ions, Proteins, and Small Molecules Using Structure-Switching Aptamers, SYBR Gold, and Exonuclease I*", Analytical Chemistry (2012), 84(8), 3554–3560. doi:10.1021/ac300690r

[22] Chalklen T., Jing Q. & Kar-Narayan S., "*Biosensors Based on Mechanical and Electrical Detection Techniques*", Sensors (2020), 20(19), 5605. doi:10.3390/s20195605

[23] Bakker, E. (2004). "*Electrochemical Sensors*". Analytical Chemistry, 76(12), 3285–3298. doi:10.1021/ac049580z

[24] Daniels J. S., & Pourmand N., "*Label-Free Impedance Biosensors: Opportunities and Challenges*", Electroanalysis (2007), 19(12), 1239–1257. doi:10.1002/elan.200603855

[25] D. Janasek, J. Franzke and A. Manz, "*Scaling and the design of miniaturized chemical-analysis systems*", Nature, vol. 442, no. 7101, pp. 374-380, 2006. Available: 10.1038/nature05059 [Accessed 15 October 2021].

[26] Watson, L. D., Maynard, P., Cullen, D. C., Sethi, R. S., Brettle, J., & Lowe, (1987). "*A microelectronic conductimetric biosensor. Biosensors*", 3(2), 101–115. doi: 10.1016/s0265-928x(87)80003-2.

[27] Nishizawa, M., Matsue, T., & Uchida, I. (1992). "*Penicillin sensor based on a microarray electrode coated with pH-responsive polypyrrole*". Analytical Chemistry, 64(21), 2642–2644. doi:10.1021/ac00045a030.

[28] Pohanka, M. (2015). "*Biosensors containing acetylcholinesterase and butyrylcholinesterase as recognition tools for detection of various compounds*". Chemical Papers, 69(1). doi:10.2478/s11696-014-0542-x.

[29] Baronas, Romas; Kulys, Juozas; Lančinskas, Algirdas; Žilinskas, Antanas (2014). "*Effect of Diffusion Limitations on Multianalyte Determination from Biased Biosensor Response*". Sensors, 14(3), 4634–4656. doi:10.3390/s140304634

[30] Ramesh, M.; Janani, R.; Deepa, C.; Rajeshkumar, L., "*Nanotechnology-Enabled Biosensors: A Review of Fundamentals, Design Principles, Materials, and Applications*". Biosensors 2023, *13*, 40. https://doi.org/10.3390/bios13010040

[31] Leva-Bueno, J., Peyman, S. A., & Millner, P. A. (2020). "*A review on impedimetric immunosensors for pathogen and biomarker detection*". Medical Microbiology and Immunology. doi: 10.1007/s00430-020-00668-0.

[32] Pohanka, M. (2018). "*Overview of Piezoelectric Biosensors, Immunosensors and DNA Sensors and Their Applications. Materials*", 11(3), 448. doi: 10.3390/ma11030448.

[33] Hundeck, H. G., Weiß, M., Scheper, T., & Schubert, F. (1993). "*Calorimetric biosensor for the detection and determination of enantiomeric excesses in aqueous and organic phases*". Biosensors and Bioelectronics, 8(3-4), 205–208. doi: 10.1016/0956-5663(93)85034-L.

[34] MEHRVAR, M., & ABDI, M. (2004). "*Recent Developments, Characteristics, and Potential Applications of Electrochemical Biosensors*". Analytical Sciences, 20(8), 1113–1126. doi:10.2116/analsci.20.1113.

[35] Chaubey, A., & Malhotra, B. D. (2002). "*Mediated biosensors*". Biosensors and Bioelectronics, 17(6-7), 441–456. doi:10.1016/s0956-5663(01)00313-x

[36] Yang, L. & Guiseppi-Elie, A. (n.d.). "*Impedimetric Biosensors for Nano- and Microfluidics*". Encyclopedia of Microfluidics and Nanofluidics, 811–823. doi: 10.1007/978-0-387-48998-8_686.

[37] **Gogoneata, S.**, Sandoiu-Ilie, A., & Morega, A. (2021). "*Numerical Simulations of the Pressure-Driven and Electrokinetic Transport in DNA Hybridization*", 2021 12th International Symposium on Advanced Topics in Electrical Engineering (ATEE), 1-4.

[38] S. Das, T. Das, S. Chakraborty, "*Modeling of coupled momentum, heat and solute transport during DNA hybridization in a microchannel in the presence of electro-osmotic effects and axial pressure gradients*", Microfluid Nanofluid, 2, pp. 37–49, 2006.

[39] D. Erickson, D. Li, U.J. Krull, "*Modeling of DNA hybridization kinetics for spatially resolved biochips*", Anal. Biochem. 317, pp. 186–200, 2003.

[40] Vaidyanathan R, Dey S, Carrascosa LG, Shiddiky MJ, Trau M. "*Alternating current electrohydrodynamics in microsystems: Pushing biomolecules and cells around on surfaces*". Biomicrofluidics. 2015 Dec 8;9(6):061501. doi: 10.1063/1.4936300. PMID: 26674299; PMCID: PMC4676781.

[41] Mercado-Borrayo, B.M. (2014). Water Reclamation and Sustainability || "*Metallurgical Slag as an Efficient and Economical Adsorbent of Arsenic*"., 95–114. doi:10.1016/B978-0-12-411645-0.00005-5.

[42] Das T, Chakraborty S., Bio-Microfluidics: Overview. "*Coupling Biology and Fluid Physics at the Scale of Microconfinement*". Microfluidics and Microfabrication. 2009 Nov 28:131–79. doi: 10.1007/978-1-4419-1543-6_4. PMCID: PMC7119918.

[43] Israelachvili N.J., "*Intermolecular and Surface Forces*", Third Edition, University of California, Santa Barbara, California, USA, 2011, ISBN 978-0-12-391927-4.

[44] P. Dutta, A. Beskok, "*Analytical Solution of Combined Electroosmotic/Pressure Driven Flows in Two-Dimensional Straight Channels: Finite Debye Layer Effects*", Anal. Chem. 2001,73, 1979-1986.

[45] Luo, Yong & Qin, Jianhua & Lin, Bingcheng. (2009). "*Methods for pumping fluids on biomedical lab-on-a-chip*". Frontiers in bioscience : a journal and virtual library. 14. 3913-24. 10.2735/3500.

[46] **S. Gogoneață**, Y. Veli and A. M. Morega, "*Numerical Analysis of Electric Field Interactions Associated with DNA Hybridization in A Microfluidic Device*", 2023 13th International Symposium on Advanced Topics in Electrical Engineering (ATEE), Bucharest, Romania, 2023, pp. 1-4, doi: 10.1109/ATEE58038.2023.10108386.

[47] Schlegel F., "*Modeling Electroosmotic Flow and the Electrical Double Layer*", october 28, 2013, https://www.comsol.com/blogs/modeling-electroosmotic-flow-electrical-double-layer/

[48] H.A. Abdulbari, E.A.M. Basheer, "*Electrochemical biosensors: electrode development, materials, design, and fabrication*", ChemBioEng Rev., 4, 2, pp. 92–105 (2017).

[49] J.I.A. Rashid, N.A. Yusof, "*The strategies of DNA immobilization and hybridization detection mechanism in the construction of electrochemical DNA sensor: A review*", Sens. Bio-Sensing Res., 16, pp. 19–31 (2017).

[50] D. Dăscălescu, C. Apetrei, "*Development of a novel electrochemical biosensor based on organized mesoporous carbon and laccase for the detection of serotonin in food supplements*", Chemosensors, 10, 9, 365 (2022).

[51] J. Contreras, V. Perez-Gonzalez, M. Mata, O. Aguilar, "*3D-printed hybrid-carbon-based electrodes for electroanalytical sensing applications*", Electrochem. Commun., 130, p. 107098 (2021).

[52] Jovic, Thomas H.; Kungwengwe, Garikai; Mills, Adam C.; Whitaker, Iain S. (2019). "*Plant-Derived Biomaterials: A Review of 3D Bioprinting and Biomedical Applications*". Frontiers in Mechanical Engineering, 5, 2019 – doi:10.3389/fmech.2019.00019

[53] L.R. Silva, A. Gevaerd, L. Marcolino Jr., M. Bergamini, T. Almeida Silva, B. Janegitz, "*3D-printed electrochemical devices for sensing and biosensing of biomarkers, Advances in Bioelectrochemistr*y", 2, pp. 121–136 (2022).

[54] **S. Gogoneață**, C. Mărculescu, A. Morega, "*Characterization of electrical properties of 3D printed biosensors with various electrode geometries*", Roum. Sci. Techn. – Électrotechn. et Énerg.Vol.68, 2, pp. 241–246, Bucarest, 2023

[55] L.R.G. Silva, J.S. Stefano, L.O. Orzari, L.C. Brazaca, E. Carrilho, L.H. Marcolino-Junior, M.F. Bergamini, R.A. A. Munoz, B.C. Janegitz, "*Electrochemical biosensor for SARS-CoV-2 cDNA detection using aups-modified 3D-printed graphene electrodes*", Biosensors, 12, p. 622 (2022).

[56] S. Handaja, H. Susanto, H. Hermawan, "*Electrical conductivity of carbon electrodes by mixing carbon rod and electrolyte paste of spent battery*", Int. J. Renew. Energy Dev., 10, 2, pp. 221–227 (2021).

[57] S.J. Bharathi, S.H. Thilagar, V. Jayasurya, "*Design of electrochemical sensor and determining the peak current of ions in solution*", IEEE International Conference on Intelligent Techniques in Control, Optimization and Signal Processing (INCOS), (pp. 1-4) IEEE, (2019)

[58] Guo, R. Lv, S. Bai, "*Recent advances on 3D printing graphene-based composites",* Nano Mater. Sci., 1, 2, p. 101-115 (2019).

[59] C. Marculescu, P. Preda, T. Burinaru, E. Chiriac, B. Tincu, A. Matei, O. Brincoveanu, C. Pachiu, M. Avram, "*Customizable fabrication process for flexible carbon-based electrochemical biosensors*", Chemosensors, 11, 4, 204 (2023).

[60] M. Xu, D. Obodo, V.K. Yadavalli, "*The design, fabrication, and applications of flexible biosensing devices, Biosens. Bioelectron*", 124–125, pp. 96–114 (2019).

[61] B. Tincu, T. Burinaru, A.-M. Enciu, P. Preda, E. Chiriac, C. Marculescu, M. Avram, A. Avram, "*Vertical graphene-based biosensor for tumor cell dielectric signature evaluation*", Micromachines, 13, 10, 1671 (2022).

[62] Verma, Neelam; Bhardwaj, Atul (2015). "*Biosensor Technology for Pesticides—A review. Applied Biochemistry and Biotechnology*", 175(6), 3093–3119. doi:10.1007/s12010-015-1489-2.

[63] Yang, L., & Guiseppi-Elie, A. (n.d.). "*Impedimetric Biosensors for Nano- and Microfluidics. Encyclopedia of Microfluidics and Nanofluidics*", 811–823. doi:10.1007/978-0-387-48998-8_686.

[64] T. A. Burinaru, B. Tincu, M. Avram, P. Preda, A.-M. Enciu, E. Chiriac, C. Mărculescu, T. Constantin, M. Militaru, "*Electrochemical impedance spectroscopy based microfluidic biosensor for the detection of circulating tumor cells*", Mater. Today Commun., 32, p. 104016 (2022).

[65] Raistrick, I.D. and J. Macdonald, "*Impedance Spectroscopy Theory, Experiment, and Applications*". A. John Wiley & Sons. Vol. Second Edition. 2005, New Jersey: A John Wiley & Sons. 1-20.

[66] Metrohm Autolab B.V., *NOVA 2.1.2. User Manual*, (2017), https://nlab.pl/uploads/edytor/User manual NOVA 2.1.pdf

[67] H. Herrera Hernández et al., "*Electrochemical Impedance Spectroscopy (EIS): A Review Study of Basic Aspects of the Corrosion Mechanism Applied to Steels*", Electrochemical Impedance Spectroscopy. IntechOpen. (2020). doi: 10.5772/intechopen.94470.